NATIONAL ADVISORY COMMITTEE FOR AERONAUTICS

TECHNICAL NOTE

No. 1694

ANALYSIS OF PLANING DATA FOR USE IN PREDICTING HYDRODYNAMIC IMPACT LOADS

By Margaret F. Steiner

Langley Aeronautical Laboratory
Langley Field, Va.

Washington

August 1948

ERRATA

NACA TN No. 1694

ANALYSIS OF PLANING DATA FOR USE IN PREDICTING HYDRODYNAMIC IMPACT LOADS
By Margaret F. Steiner

August 1948

ERRATA

Page 5, line 4: This line should be changed to read as follows:
"where $m_s = \frac{Ky^2}{\cos^2\tau}$ corrected for end loss and $V_p = V_n \cot \tau$. This"

Page 11, under section entitled "Results": Change the last line of the first paragraph to read "a function of trim in figure 5."

Page 12, second paragraph under "Chines Immersed," lines 5 and 9: Reference should be to figure 6 instead of figure 5.

Page 14, next to last line: Figure 4 should be figure 3.

Page 35, figure 8: Sin τ should be omitted from the formula for C_g. 30°

-- the water load is defined as the rate at which momentum is imparted to the downwash or the product of the momentum in a transverse plane at the step and the velocity of the fluid along the keel relative to the

NATIONAL ADVISORY COMMITTEE FOR AERONAUTICS

TECHNICAL NOTE NO. 1694

ANALYSIS OF PLANING DATA FOR USE IN PREDICTING HYDRODYNAMIC IMPACT LOADS

By Margaret F. Steiner

SUMMARY

An analysis is made of planing data covering a wide range of dead-rise angles, trims, speeds, and beam loadings. General hydrodynamic-impact-load equations are applied to the planing float and corrections are made to the theoretical nondimensional coefficients which are used in defining the effect of the apparent additional mass associated with the immersed body in order to obtain agreement with experimental planing data. The analysis is divided into three phases in which the inertia force is determined by evaluating data from tests in which the chines are above level water and the buoyant force is negligible, data from tests in which the chines are above level water and the buoyant force is significant, and data from tests in which the chines are immersed with buoyant and steady-flow forces included.

The results of the analysis include equations for the inertia force which contain correction factors to compensate for the effect of gravity upon the growth of the apparent additional mass at low Froude numbers. Summary equations for the total water reaction are obtained from the three phases of the analysis and are found to give excellent agreement with experimental planing data for dead-rise angles between 10° and 40°. The planing coefficients and gravity correction factors which are included in the resultant equations may be substituted directly in the general hydrodynamic-impact-load equations for angles of dead rise between 10° and 30° if the buoyant and steady-flow forces, considered in the analysis of planing data, are also used and if the effect of gravity at different Froude numbers, indicated by the analysis of planing data, is assumed to be unaffected by the accelerations which occur during impact.

INTRODUCTION

The magnitude of hydrodynamic loads experienced by seaplanes during a landing impact has been investigated experimentally and theoretically by the National Advisory Committee for Aeronautics. The results as reported in references 1 and 2 provide a rational means of determining loads on conventional V-bottom hulls in a step landing. One component of the water load is defined as the rate at which momentum is imparted to the downwash or the product of the momentum in a transverse plane at the step and the velocity of the fluid along the keel relative to the

immersing body. The momentum in the plane at the step was defined as the product of an apparent additional mass associated with the float cross section and its instantaneous velocity in a direction normal to the keel of the float. In reference 1 it was pointed out that non-dimensional coefficients used in defining the apparent additional mass for different float configurations could be obtained by an analysis of data from planing tests, and limited data for one angle of dead rise were analyzed. Since appreciable planing data are available covering a wide range of dead-rise angles, trims, speeds, and beam loadings, the analysis is extended to include these data in order to obtain more suitable coefficients which may be used in determining the apparent additional mass over a wider range of float geometry and Froude numbers than that previously investigated in impact-basin tests.

The analysis of planing data was accomplished by introducing the experimental results into the general hydrodynamic equations of reference 2 as applied to the planing float. The analysis has been divided into three phases which include data from high-speed planing tests with chines above level water, data from low-speed planing tests with chines above level water, and data from tests with high beam loadings and chines immersed. In the first phase of the analysis, data are presented from high-speed tests in which a seaplane impact at high Froude numbers was simulated. Buoyant forces are considered insignificant and empirical corrections are made to the cited equations, which define the inertia force, in order to obtain agreement with planing data. In the second phase of the analysis, buoyant forces are considered and the effect of gravity on the apparent additional mass at low Froude numbers is determined. In the third phase of the analysis, the data from tests in which the chines were immersed are assumed to correspond to the immersion of a float or planing device with high beam loading. For this phase buoyant forces and inertia forces are included and, in addition, steady-flow forces are defined which arise from the flow of water around the area that is submerged aft of the intersection of the chines with level-water line.

The ultimate purpose of the present analysis is to determine the effective apparent additional mass over the extended range of float geometry and Froude numbers for which planing data are available. Incidental to the calculation of effective mass is the computation of steady-flow and buoyant forces, which are considered separately in order to isolate the inertia forces and, thus, to determine the effect of gravity and the effect of chine immersion upon the effective apparent additional mass associated with the float bottom.

SYMBOLS

Consistent units must be used in all cases.

A	ratio of length to mean beam of hull

b	beam in plane of undisturbed water surface
B	beam of float (from chine to chine)
C_p	planing load coefficient
c	wetted semiwidth at the step
dl	increment of length along keel
f	function of two-dimensional Froude number $\frac{(V_n)^2}{gb}$ and trim $\left(f = \frac{\left(\frac{b}{2}\right)^{1/2}}{V}\right)$
F	total computed vertical water force balancing weight of model
F_e	effective fluid inertia force which deflects stream of water; this force is due to expanding mass on wedge with triangular projection, vertical unless appearing with subscript; subscript n normal to keel, p applied to an individual transverse plane
F_e'	corrected value of F_e
F_b	vertical component of buoyant force
F_s	vertical component of steady-flow force which acts on area submerged behind intersection of chines with water surface
l	wetted length along keel
m_s	two-dimensional apparent additional mass in plane at step normal to keel
m	slope of empirical gravity correction curves
V	horizontal velocity
V_n	velocity normal to keel
W	actual load on model
y	draft of keel at step, normal to water surface
z	penetration of step normal to keel
Z	depth of float cross section from chine to keel (measured normal to keel)

β angle of dead rise

ϵ angle of downwash

$f(\beta)$ variation of angle of dead rise

$f'(\beta)$ alternate function of angle of dead rise

$\phi(A)$ end-loss factor

ρ mass density of water (Weight of water for tests from which planing data were obtained was considered as 63.5 lb/cu ft.)

τ trim angle

Subscripts:

1 in plane 1-1
2 in plane 2-2

ANALYTICAL CONSIDERATIONS

The flow processes beneath a wedge penetrating the water surface have been discussed in references 1 and 2. The inertia forces arising from the immersion are defined as being equal to the rate of change of momentum in the flow planes beneath a wedge and are obtained by summing the forces in individual transverse flow planes. The reaction in a plane of incremental length dl is defined in terms of the momentum in the plane as

$$F_{e_p} = \frac{d}{dt}\left(Kz^2 dl \frac{dz}{dt}\right) \tag{1}$$

which is similar to that given in equation (21) of reference 1 where s is replaced by l. In equation (1) K is a theoretical coefficient that depends upon the dead-rise angle. The integration of the individual forces over the wetted length provides an equation for the total water reaction normal to the keel based on the measured drafts. This equation is

$$F_{e_n} = \frac{Ky^3 \frac{dV_n}{dt}}{3 \sin \tau \cos^2 \tau} + \frac{Ky^2 V_n^2}{\sin \tau \cos \tau} \tag{2}$$

For the case of the planing float the first term of equation (2) is zero and the second term represents the rate at which the momentum is

imparted to the downwash in connection with the flow planes sliding off the step. This term may be generalized as

$$F_{e_n} = m_s V_n V_p \tag{3}$$

where $m_s = Ky^2$ corrected for end loss and $V_p = \frac{V_n}{\sin \tau \cos \tau}$. This fundamental equation is used throughout the three phases of the analysis, which were mentioned in the introduction, with the principal objective being the evaluation of the two-dimensional apparent additional mass m_s for different dead-rise angles and for different Froude numbers. The conditions which are considered in defining the total water reaction for the different phases of the analysis are given in the sections to follow.

Chines above Level Water

Planing at high speeds.- In the analysis of data from planing tests at high Froude numbers, the inertia force which is the only force that balances the weight is based on the following generalized equation for the two-dimensional apparent additional mass:

$$m_s = \frac{\pi}{2}\rho z^2 f(\beta) \tag{4}$$

which is similar to that given in equation (1) of reference 2 in which $f(\beta)$ appears in the form of $\left[f(\beta)\right]^2$. Equation (4) is substituted into equation (3) and the vertical component of the inertia force is expressed in terms of the horizontal velocity V; thus

$$F_e = \frac{\pi}{2} f(\beta)\rho z^2 V^2 \cos^2\tau \sin \tau$$

Since the draft is usually the measured quantity, the equation for the inertia force when corrected for end losses which occur for the three-dimensional case is expressed in terms of y as

$$F_e = W = \frac{\pi}{2} y^2 f(\beta)\phi(A)\rho V^2 \sin \tau \tag{5}$$

or in terms of the beam at the step in the plane of level water as

$$F_e = W = \frac{\pi}{2}\left(\frac{b}{2}\right)^2 \frac{f(\beta)}{\cot^2\beta}\phi(A)\rho V^2 \sin \tau \cos^2\tau \tag{6}$$

These equations may be better understood if the concept sometimes used in interpreting the lift on a wing is considered and a cylindrical stream having a diameter equal to the wing span is considered to be deflected through an angle of downwash and the lift to be that force which is exerted in deflecting the mass. In applications to the planing float the fact that forces are acting only on the lower surface of the float reduces the mass to a semicylinder. As shown in figure 1(a) and 1(b), the loaded cross section is greater than the cross section below level water because of a transverse "pile up" of water which is indicated by the shaded area. The effect of this additional area is considered to be a growth of effective beam or span. In other words, the semicircular cross section used in computing the apparent additional mass is $\frac{\pi}{2}c^2$ where c is the semiwetted beam at the top of the pile-up. In terms of Wagner's function of dead rise $\left(\frac{\pi}{2\beta}-1\right)^2$, which has been used in references 1 and 2, the semiwetted beam c is equal to $\left[\frac{\left(\frac{\pi}{2\beta}-1\right)^2}{\cot^2\beta}\right]^{1/2}\frac{b}{2}$. For large ratios of length to beam in which the value of $\phi(A)$ approaches unity, the angle of downwash ϵ would be equal to the trim. The function $\phi(A)$, based on Pabst's factor $1-\frac{1}{2A}$, is used as a correction factor which may be considered as indicative of the difference between the angle of downwash and the trim. For the planing float with chines above level water

$$A = \frac{\tan\ \beta}{\tan\ \tau}$$

Introducing the aforementioned factors into equation (5) gives

$$F_e = W = \frac{\pi}{2}y^2\left(\frac{\pi}{2\beta}-1\right)^2\left(1-\frac{\tan\ \tau}{2\tan\ \beta}\right)\rho V^2 \sin\ \tau \qquad (7)$$

This equation may be transposed to carry those concepts that are most adaptable to experimental measurements on the left-hand side; thus

$$\frac{W}{\rho V^2 y^2} = \left(\frac{\pi}{2\beta}-1\right)^2\left(1-\frac{\tan\ \tau}{2\tan\ \beta}\right)\frac{\pi}{2}\sin\ \tau$$

The right-hand side of the equation is a nondimensional planing load coefficient conveniently designated C_p based only on the float shape and trim. Agreement is obtained by omitting Wagner's dead-rise function $\left(\frac{\pi}{2\beta}-1\right)^2$ and deriving a different function $f'(\beta)$ so that equation (5) becomes

$$F_e' = W = \frac{\pi}{2} y^2 f'(\beta) \phi(A) \rho V^2 \sin \tau \tag{8}$$

Planing at low speeds.— In planing at low speeds where buoyant forces comprise more than 10 percent of the total water reaction, the possibility arises that gravity may affect the apparent additional mass which is associated with the immersed wedge. As previously mentioned, the total inertia reaction exerted on a float is obtained by the integration of the reaction in individual flow planes along the length of the float. This procedure implies that the flow pattern is the same in all planes and at all speeds but the laws of dynamic similitude state that this hypothesis is valid only at the same Froude number. Since the Froude number is proportional to the ratio of the inertia forces to the buoyant forces, it is reasonable to assume that similitude is attained until the buoyant forces become appreciable. The analysis of data from tests made at low Froude numbers in which buoyant forces are important is carried out with a function of Froude number as the significant parameter.

The water reaction balancing the weight of the model is defined as

$$F = W = F_e' + F_b \tag{9}$$

The inertia force F_e' is given by equation (8). The buoyant force F_b shown in figure 1(c), when based on the draft, becomes

$$F_b = \frac{\rho g y^3}{3 \sin \tau \tan \beta} \tag{10}$$

The ratio $\frac{W - F_b}{F_e'}$ is considered as an empirical gravity correction factor C_g and its variation with a function f based on Froude number and trim is determined. Empirical curves giving this variation are obtained in which C_g changes from unity as gravity effects become important at different Froude numbers. These curves are used in conjunction with equation (9) to give

$$F = W = F_e' C_g + F_b \tag{11}$$

and using equations (8) and (10) with equation (11) provides an expression for the total water reaction which is applicable for all Froude numbers for a planing wedge with chines above level water. Thus,

$$F = W = \frac{\pi}{2} y^2 f'(\beta) \phi(A) \rho V^2 \sin \tau \, C_g + \frac{\rho g y^3}{3 \sin \tau \tan \beta} \tag{12}$$

Chines Immersed

The analysis of data in which the chines at the step become immersed is made according to two concepts. In both concepts the water reaction which balances the weight is defined as

$$F = W = F_e' + F_b + F_s \tag{13}$$

In figure 2 the various forces are shown as acting on a wedge with chines immersed. As seen in figure 2(b) the total fluid inertia force may be based on the concept that the maximum cross-sectional area of the apparent additional mass is in plane 1-1 so that the draft to be used in equation (5) is equal to $\frac{\cot \beta}{[f'(\beta)]^{1/2}} Z \cos \tau$. On the other hand, the total fluid inertia force may be based on the apparent additional mass in plane 2-2 where the draft used in equation (5) is the full draft $Z \cos \tau$.

The fluid inertia force is defined according to which concept is used in determining the two-dimensional apparent additional mass. For two-dimensional apparent additional mass in plane 1-1

$$F_{e'_1} = \frac{\pi}{2}\left(\frac{\cot \beta}{[f'(\beta)]^{1/2}} Z \cos \tau\right)^2 f'(\beta)\phi(A)\rho V^2 \sin \tau \tag{14}$$

and for two-dimensional apparent additional mass in plane 2-2

$$F_{e'_2} = \frac{\pi}{2}(Z \cos \tau)^2 f'(\beta)\phi(A)\rho V^2 \sin \tau \tag{15}$$

In these equations $\phi(A)$ is based on the total projected area S, as shown in figure 2(a), so that $A = \frac{l^2}{S}$.

The buoyant force shown in figure 2(c) is represented for both concepts by an approximate equation obtained by summing the weight of water contained in volumes (1) and (2) (fig. 2(c)). If $\sin \tau$ is assumed to be equal to $\tan \tau$, then

$$F_b = \frac{\rho g Z}{\sin \tau \tan \beta}\left(y^2 - Zy + \frac{Z^2}{3}\right) \tag{16}$$

The steady-flow force shown in figure 2(d), which is basically the product of dynamic pressure induced by a stream of water impinging normal to the keel and the area upon which it acts as discussed in reference 3,

is defined according to which plane is taken as the beginning of chine immersion; that is, if plane 1–1 is used,

$$F_{s_1} = C_{s_2}\frac{\rho}{2}bV^2\left(y - \frac{\cot \beta}{[f'(\beta)]^{1/2}}Z \cos \tau\right)\sin \tau \cos \tau \qquad (17)$$

or, if plane 2–2 is used,

$$F_{s_2} = C_{s_2}\frac{\rho}{2}bV^2(y - Z \cos \tau) \sin \tau \cos \tau \qquad (18)$$

The values for C_s, which is Bobyleff's dead-rise correction factor, are presented in table I. (See reference 3, p. 105.)

By use of the concept in which the apparent additional mass is based on plane 1–1, equations (14), (16), and (17) are substituted in equation (13). The ratio $\frac{W - F_b - F_{s_1}}{F_{e'_1}}$ is considered as a gravity correction factor C_g and its variation with the function f of Froude number and trim is determined.

By use of the concept in which the apparent additional mass is based on plane 2–2, equations (15), (16), and (18) are substituted in equation (13). The expression for the inertia force given by equation (15), however, is corrected by the empirical Froude correction curves that were obtained in the analysis of data for chines above level water. The equation that defines the total water reaction and is used in evaluating experimental data for the case in which chines are below level water finally becomes

$$F = W = \frac{\pi}{2}(Z \cos \tau)^2 f'(\beta)\phi(A)\rho V^2 \sin \tau \, C_g + C_{s_2}\frac{\rho}{2}bV^2(y - Z \cos \tau)\sin \tau \cos \tau + \frac{\rho g Z}{\sin \tau \tan \beta}\left(y^2 - Zy + \frac{Z^2}{3}\right) \qquad (19)$$

SCOPE AND PRECISION OF DATA

Chines above Level Water

In the first and second phases of the analysis in which the chines are above level water, experimental data from references 4 and 5 together with some other data obtained from recent tests made in Langley tank no. 2 are used for comparison with theory. The data which are analyzed were

obtained with planing plates having dead-rise angles of 10°, 20°, 22½°, and 30°, trims between 2° and 10°, and ratios of length to mean beam between 1.25 and 8.35. Pertinent geometric properties of the planing plates or floats are listed in table II.

The data from references 4 and 5 are shown in figure 3 as curves of y plotted against $\frac{1}{V}$ for the different loads, trims, and dead-rise angles. The draft at chine immersion $Z \cos \tau$ is noted on the ordinate of each plot. The drafts from reference 4 are computed from the trims and wetted lengths which are given in tables II, III, and IV, and figures 7 to 18 of this reference since a great deal of scatter is evident in the measured drafts. At the high speeds, also, the measured drafts are not considered to be reliable because of the method used in obtaining them (reference 6). Since no wetted lengths are given in reference 5, the recorded drafts are used but the great scatter in the data permits only a rough comparison with computed values. Also, the data presented in reference 5 is further complicated by the presence of a pulled-up bow and an afterbody that limit the amount of data which is usable to the few runs involving the prismatic section alone.

The unpublished data from recent tests conducted in Langley tank no. 2 were obtained by a method having more accurate draft measurements. The general test procedure followed is the same as that discussed in reference 6 and a part of these results is given in table III. Data for the case in which the chines are above level water are presented in figure 3(b) for comparison with data based on wetted length from reference 4, in which a similar planing plate having a different beam was used.

The precision of the analysis is dependent upon the accuracy of the experimental data which are used and upon establishing the accuracy of the experimental data insofar as they are used in the analysis. In figure 3 the accuracy of a particular draft is observed to vary with speed; that is, at the higher speeds the drafts are small and the percentage errors may be large. Because a large number of points are available for each loading condition, the mean curve defined by a set of experimental points is considered to be accurate within a range of ±5 percent with the exception of figure 3(d) which, as previously mentioned, contains data from tests involving a float with peculiar geometric properties and a method of measurement that results in undue scatter in the data. In this case the mean curve is considered to be accurate within a range of ±10 percent. For computations in which the draft is squared or cubed, the accuracy of the experimental quantities is approximately 10 and 15 percent, respectively. The quality of agreement between the experimental and computed results which are referred to in the discussion is in all cases consistent with the precision of the experimental data which has been discussed in the present section.

Chines Immersed

For the third phase of the analysis, data from references 4 and 7 and several test points obtained in the recent tests previously mentioned were used. These data covered dead-rise angles of 10°, 20°, 30°, and 40°, trims between 2° and 11°, and ratios of length to mean beam between 1.25 and 12.00.

The data from reference 4 are included in figure 3 as indicated by the points above $y = Z \cos \tau$; the data from reference 7 are presented in table IV. The pertinent geometric properties of the planing devices used in obtaining these data are given in table II.

The accuracy of the draft measurements which are used in the present analysis is considered to be approximately ±5 percent. In the case of chine immersion the inertia force is virtually independent of draft by buoyancy and is expressed as a quadratic equation in terms of the measured draft so that the force is accurate within ±10 percent. The quality of agreement of experimental and computed results, which is referred to in the discussion, for the case of chine immersion is based on these values.

RESULTS

Chines above Level Water

Check computations are made in order to assort the data according to the magnitude of the buoyant force. The values of the buoyant force as computed for planing plates having beams of 1.33 feet and dead-rise angles β of 10°, 20°, and 30° are presented in figure 4. For drafts less than one-half the depth of the float $\left(y < \frac{Z}{2} \cos \tau\right)$, the force is usually less than 10 percent of the total water reaction. On the basis that the inertia force defined in equation (5) is the only significant force for these low drafts, lines are drawn through the origin and tangent to the mean of the experimental curves described by the test points of $y < \frac{Z}{2} \cos \tau$ that are given in figure 3 in order to obtain the product Vy which is the slope of each tangent. The slopes are introduced into equation (7) and the experimental results are shown as a function of trim.

The theoretical coefficient C_p which is included in equation (7) contains a dead-rise function $\left(\frac{\pi}{2\beta} - 1\right)^2$ which has been used in the general impact equations of references 1 and 2. The variation of the coefficient C_p with trim is shown by the dashed-line curves of figure 5. An alternate dead-rise function $1.42 \cot^2\beta$ is substituted in the equation in place of $\left(\frac{\pi}{2\beta} - 1\right)^2$ and the variation of the altered coefficient is shown by the solid-line curves of figure 5.

In the second phase of the analysis, in which buoyancy is significant, the measured drafts are used in conjunction with equation (9) and the empirical gravity correction factor $\frac{W - F_b}{F_e}$ or C_g is plotted against the function f. (See fig. 6.) A linear equation is written for a mean line through the experimental scatter for each dead-rise angle as an approximation of the effect of gravity at different Froude numbers. By use of these curves with equation (12), drafts are assumed and solutions are made for values of $\frac{1}{V}$ so that theoretical curves of y plotted against $\frac{1}{V}$ are obtained, which are given in figures 3(a), 3(b), and 3(c) as indicated by the solid lines that extend from $y = 0$ to $y = Z \cos \tau$ for the case in which the chines are above level water.

Chines Immersed

Data from reference 4 are evaluated by use of the first concept in which the apparent additional mass is based on the semicircular cross section shown in plane 1-1 (fig. 2(b)). The variation of the empirical gravity correction factor C_g, which is obtained by use of equations (14), (16), and (17), with the function of Froude number f is shown in figure 7. The corresponding curves that were given in figure 6 for the case in which chines are above level water are also included in figure 7 for purposes of comparison.

The second concept, in which the apparent additional mass is based on the semicircular cross section of plane 2-2 in figure 2(b), is also used and equations (15), (16), and (18) are used in obtaining the over-all water load. In this concept equation (15), which defines inertia force, is corrected for gravity effects by use of the curves of figure 5. (The reason for making this correction will be discussed subsequently.) By use of equation (19), which contains the total water reaction, solutions are made for values of y plotted against values of $\frac{1}{V}$ by substituting the linear equations for C_g, which are indicated in figure 5, in equation (19). These theoretical curves are shown by the extended solid-line curves in figures 3(a), 3(b), and 3(c), beginning at $y = Z \cos \tau$ (the draft at chine immersion) and extending through the range of the experimental drafts.

A final comparison of experimental and theoretical results for the case of chine immersion is made by using the data from reference 7 and the unpublished data in addition to that already considered from reference 4. The empirical curves of figure 7 are altered by introducing an arbitrary dead-rise function $\cot \beta$ into the abscissa, as presented in figure 8, in order to spread the empirical lines apart and thus permit more accurate interpolations for angles of dead rise between 10° and 40°. Limited experimental data for a dead-rise angle of 40° (given in table IV) were used to locate the empirical line representing the gravity effect on

the apparent additional mass for that angle of dead rise; as in previous cases, the apparent additional mass was based on a beam 20 percent greater than the actual beam of the plate. The total water reaction is obtained by use of these curves with equation (19). The comparison between experimental and computed loads is made on the basis of $\left(F/F_b\right)^{1/2}$ as compared with $\left(W/F_b\right)^{1/2}$ in order to provide a means of readily seeing the points that were those for which the inertia forces are most significant, namely, the higher values of $\left(W/F_b\right)^{1/2}$ and the values in which buoyancy comprises a principal part of the total reaction (values $\doteq 1.0$). The square root is extracted since the computed values used in obtaining the inertia and the buoyant forces are based on the square of the velocity and draft, respectively; the scatter which appears in figure 9 and the experimental scatter in the measured quantities are of comparable magnitudes. The plot was made on logarithmic paper in order to spread the points apart for more convenient inspection of the agreement between the experimental and theoretical quantities.

DISCUSSION

Chines above Level Water

Planing at high speeds.- The results of the analysis of data from high-speed planing tests in which the chines are above level water (fig. 5) indicate that the impact equations of references 1 and 2 as applied to the planing float appear to be adequate as far as end losses are concerned since no disagreement with trim is noticeable but are inadequate with regard to the dead-rise-angle correction factor. The values of curves given by the coefficient $\frac{\pi}{2}\left(\frac{\pi}{2\beta}-1\right)^2\phi(A)\sin\tau$ used in reference 2 and indicated by the dashed-line curves of figure 5 are higher than corresponding experimental values of $\frac{W}{\rho V^2 y^2}$ at a dead-rise angle of 10° and are lower at a dead-rise angle of 30°. In order to obtain a more suitable dead-rise-angle factor, equation (6) is used in terms of the beam rather than in terms of the draft. When the term $\frac{f(\beta)}{\cot^2\beta}$ is omitted from this equation and the experimental values are substituted, an empirical constant 1.42 is found to be required for agreement between theoretical and experimental results; that is

$$\frac{W}{\rho\left(\frac{b}{2}\right)^2 V^2} = 1.42\,\frac{\pi}{2}\,\phi(A)\sin\tau\cos^2\tau$$

If the constant is substituted in equation (6) and if equation (6) is changed to an equivalent expression in terms of the draft as in equation (5), $f'(\beta)$ is found to be numerically equal to $1.42 \cot^2\beta$. The theoretical coefficient C_p, which incorporates $f'(\beta)$ as indicated by the solid-line curves of figure 5, is in excellent agreement with the experimental results also presented in figure 5.

The altered dead-rise function $1.42 \cot^2\beta$, used when the equations are based on the measured draft, is obviously not valid for a flat plate; therefore, rather than consider the term as a dead-rise factor further observations are referred to equation (6), based on the beam, in which $\cot^2\beta$ is canceled out. The inertia force is seen to be independent of the dead-rise angle except for end-loss corrections. If the factor 1.42 is considered as a wave-rise factor, then the results of planing analysis indicate that a constant wave rise of 20 percent should be considered in computing the apparent additional mass for all angles of dead rise.

In figure 5 the computed values based on equation (5), in which $1.42 \cot^2\beta$ has been substituted, are observed to be in agreement with the experimental values within ±10 percent. Since this range of accuracy is of the same magnitude as the optimum accuracy of the experimental quantity, which is dependent upon the measured draft, the agreement of the following equation with experimental data for the case of planing at high speeds is considered excellent:

$$F_e' = W = \frac{\pi}{2}\left(1.19\,\frac{b}{2}\right)^2\left(1 - \frac{\tan\tau}{2\tan\beta}\right)\rho V^2 \sin\tau\,\cos^2\tau \qquad (20)$$

or, if based on the draft,

$$F_e' = W = \frac{\pi}{2}(1.19y)^2\cot^2\beta\left(1 - \frac{\tan\tau}{2\tan\beta}\right)\rho V^2 \sin\tau \qquad (21)$$

Planing at low speeds.- For planing at low speeds buoyant forces becomes appreciable, and the effect of gravity upon the flow pattern at low Froude numbers makes necessary the correction of equations (20) and (21) to compensate for the gravity effects. The results given in figure 6 show that gravity correction factors as low as 0.4 are required in some cases. The correction factors that are to be used with these equations are found to vary linearly with a function of Froude number and trim as shown in figure 6. These empirical lines appear to be clearly defined since the scatter of experimental data is limited; that is, the apparent-additional-mass coefficient corrected by the empirical factor is accurate within the desired limits of ±10 percent. As seen in figure 4 the use of the empirical correction curves and equation (12) appears to be adequate since the theoretical and experimental curves of y

plotted against $\frac{1}{V}$ are in very good agreement up to the draft of chine immersion.

The differences between computed and experimental loads at low Froude number have been attributed to the effect of gravity on the inertia force. In the derivation of the inertia force the assumption is made that flow similarity exists in all cases; that is, every plane beneath the float is assumed to be similar to every other plane regardless of the draft or the speed. According to the laws of similitude this assumption is not valid, and the analysis of planing data has yielded reasonable correction curves which show the effect of gravity as changing the flow pattern and thus reducing the inertia loads. The effect of gravity may be that the wave caused by the displaced water spreads out transversely and, thus, that the local pressures are reduced and in turn the effective apparent-additional-mass term is reduced.

For a given angle of dead rise, some longitudinal spreading of the wave is likely to occur; therefore, the gravity effect is greater at higher trims. This fact has been taken into account by using the horizontal velocity rather than the normal velocity in the function of Froude number. In other words, in order to condense the trim effects, $\sin \tau$ is used with the reciprocal of the square root of Froude number $\left(\frac{gb}{V_n^2}\right)^{1/2}$ to give a proportional function f equal to $\frac{\left(\frac{b}{2}\right)^{1/2}}{V}$.

For a given trim, the gravity effects are likely to be more pronounced at higher dead-rise angles at which buoyant forces are higher in proportion to the inertia forces and Froude numbers are lower. The exact variation of the gravity effect with angle of dead rise is not clear since only three angles of dead rise are considered and the arbitrary dead-rise factor $\cot \beta$, which is introduced into the abscissa in figure 8 for ease in interpolating and extrapolating between and beyond angles of 10° to 30°, has no particular physical meaning.

The final equation which provides excellent agreement for the planing float with chines above level water at all Froude numbers is

$$F = W = \frac{\pi}{2}(1.19y)^2 \cot^2\beta\left(1 - \frac{\tan \tau}{2 \tan \beta}\right)\rho V^2 \sin \tau \; C_g + \frac{\rho g y^3}{3 \sin \tau \tan \beta} \quad (22)$$

Chines Immersed

In the analysis of data for the case with chines immersed (based on the first concept in which the apparent additional mass is determined from plane 1-1 of fig. 2(b)), the results given in figure 7 show that the empirical gravity corrections are about 40 percent greater than those given by the analysis of data with chines above level water for all values of f. Furthermore, when the values of f are low enough to indicate negligible gravity effects (see fig. 7), the computed inertia

forces are in disagreement with experimental values by about 40 percent. This difference is noted to be approximately that which exists between the inertia force given by equation (14) and that which corresponds to the second concept given by equation (15). This difference is due to the fact that the drafts to be used in equations (14) and (15) are $y = \frac{1}{1.19}Z \cos\tau$ and $y = Z \cos\tau$, respectively, and, since the drafts are squared, the resulting difference in inertia force is about 40 percent. Because of these observations, the analysis of the data by the concept in which the apparent additional mass is determined from plane 2-2 of figure 2(b) is used, and the gravity correction curves in figure 6 are directly applied to the inertia force defined in equation (15). The theoretical curves showing the variation of y with $\frac{1}{V}$ that are obtained by using equation (19), which defines the total water reaction as based on the second concept, are in excellent agreement with the corresponding experimental curves of figure 3. The final comparison of computed and experimental values of $\left(F/F_b\right)^{1/2}$ and $\left(W/F_b\right)^{1/2}$, which is given in figure 9, indicates very good agreement for angles of dead rise between 10° and 40° since the scatter is about the same as the experimental range of accuracy of ±5 percent.

The final equation that provides very good agreement with experimental results for the case of chine immersion is

$$F = W = \frac{\pi}{2}(1.19Z\cos\tau)^2\cot^2\beta\left[1 - \frac{Z\sin\tau\left(y - \frac{Z}{2}\right)}{y^2\tan\beta}\right]\rho V^2\sin\tau\, C_g$$

$$+ C_s\frac{\rho Z}{\tan\beta}V^2(y - Z\cos\tau)\sin\tau\cos\tau + \frac{\rho g Z}{\sin\tau\tan\beta}\left(y^2 - Zy + \frac{Z^2}{3}\right) \qquad (23)$$

Applicability of Results to Hydrodynamic Theory

Chines above level water, high Froude number.- The analysis of planing data permits a simpler and basically more accurate means of obtaining the nondimensional coefficients that are used in defining the apparent additional mass for use in general impact equations such as those given in references 1 and 2. In determining the applicability of results of the analysis of planing data at high Froude numbers which correspond to the condition that has been considered in impact work, the difference between the planing coefficient shown by the solid-line curves of figure 5 and the corresponding impact coefficient shown by the dashed-line curves is observed to be due to the difference in the dead-rise-angle factors. The planing coefficient includes the alternate dead-rise

function $1.42 \cot^2\beta$; whereas the impact coefficient includes Wagner's dead-rise function $\left(\frac{\pi}{2\beta} - 1\right)^2$. If these respective terms are used to compute the effective beam which must be considered in computing the apparent additional mass, the former term implies an effective beam 20 percent greater than the actual beam for all dead-rise angles and the latter term implies a ratio of effective beam to actual beam which varies with dead-rise angle.

The planing coefficient has been found to be in agreement with extensive planing data for chines above level water for angles of dead rise between 10° and 30°; whereas the impact coefficient has been shown in reference 2 to be in agreement with extensive experimental impact data for angles of dead rise between $22\frac{1}{2}^\circ$ and 40°. For an angle of dead rise between 20° and 30° for which both planing and impact experimental data are available, the difference between the coefficients is only 5 to 8 percent. The corresponding difference in the maximum load-factor coefficients, which are obtained in reference 2 and based on the respective coefficients, is less than 2 percent; therefore, either factor may be used. In references 1 and 2 a statement is made to the effect that the use of Wagner's function $\left(\frac{\pi}{2\beta} - 1\right)^2$ is questionable for dead-rise angles less than 15°, so that it is reasonable to believe that the true dead-rise function may approach the value $1.42 \cot^2\beta$; this function is in agreement with planing data for an angle of dead rise of 10°. No planing data are available for a planing plate with a dead-rise angle of 40° and chines above level water and, therefore, no explanation can be made of the difference in proposed coefficients at that angle. The true dead-rise variation may possibly approach Wagner's factor which when used to compute the wave rise implies that no wave rise exists at a dead-rise angle of 45° so that the effective beam is the beam in the plane of the level water surface.

Chines above level water, low Froude number.— Insofar as the application of the results of the analysis of planing data for low Froude numbers to the impact case for dead-rise angles between 10° and 30° is concerned, it is believed that the empirical gravity corrections may be applied directly to the apparent-additional-mass term if the fact is accepted that the discrepancies in the computed and experimental planing loads are due only to gravity effects upon the inertia load and that impact accelerations which are absent in the planing problem are independent of the effects of gravity upon the apparent additional mass. The buoyant force that has been defined on the basis of displaced water may possibly be incorrect since negative pressures in the water acting on the part of the plate above the level water line may act upon the plate in such a manner as to balance part of the positive buoyant pressures that act below level water. Although results of the analysis of planing data shown in figures 6 and 7 clearly called for a correction which is a function of velocity for a given draft, other possibilities

were not considered inasmuch as the agreement that is obtained by using the empirical gravity correction curves of figures 6 and 8 appears to be entirely satisfactory for the planing case.

Chines immersed.— The results of the analysis of planing data for the case of chine immersion show that the maximum cross section used in computing the apparent additional mass should be based on a diameter which is 20 percent greater than the maximum beam in the plane of level water for all angles of dead rise. This fact is contrary to the proposed theory of reference 2 in which the apparent additional mass was based on the actual beam and very limited impact data were offered for the case of chine immersion to support this concept. In both the impact and planing equations the apparent additional mass for the case in which the chines are immersed is found to be independent of dead-rise angle except for the end-loss factor, but the apparent additional mass which is indicated by planing data is 40 percent greater than that given by the impact equations. Appreciable planing data for dead-rise angles between 10° and 30° and limited planing data for a dead-rise angle of 40° were shown to be in good agreement with the planing equations. Since the planing plates had no vertical sides above the sharp edges at the chines, "spilling over" may have occurred in tests with chines immersed; in this case the apparent weight would be increased and an increase in the inertia force such as the 40-percent value might be called for. Although the gravity correction factors for the case of chine immersion coincided with corresponding curves for the case in which the chines were above level water when the 40-percent increase in the inertia force was included, the results of the planing analysis are believed to be directly applicable to the impact equations for computing the maximum loads on a V-shaped plate such as a hydroflap. Further correlation of impact and planing tests is necessary to determine the applicability of the results to the case of a float or hull with vertical sides extended upward from the chines.

RECOMMENDATIONS FOR FUTURE RESEARCH

Further planing tests should be made to obtain a check of the data used herein and to obtain more complete data over a wider range of dead-rise angles and ratios of mean length to beam. In particular, since neither the planing nor impact coefficients as presented in figure 5 are valid for the flat plate, the proper coefficient for this end point should be determined. In future tests more accurate measurements of draft and velocity are required to refine further the equations presented herein. In particular, the accuracy of the instantaneous draft should not be less than ±2 percent. In future tests the magnitude and shape of the wave rise and the variation with speed should be investigated. Local pressure measurements should be obtained since they will aid in a clearer understanding of the effect of gravity upon the flow pattern. Finally, a correlation between planing and impact data should be made for the triangular cross section, and tests should be made with and without vertical

sides extending upward from the chines. Once the applicability of planing data for defining the apparent additional mass to be used in impact theory for a triangular cross section is verified over a wide range of test conditions, planing tests with a variety of cross sections can be used to define the apparent-additional-mass term and impact tests would be considerably simplified in that only check points would be needed to verify the apparent-additional-mass term.

SUMMARY OF EQUATIONS

The equations defining the water reaction on a planing float have been shown to be in very good agreement with planing data for dead-rise angles between 10° and 40° and for ratios of mean length to beam greater than 1.25; they are given herein in summary.

The vertical water reaction for the planing wedge with chines above level water as based on the measured draft is expressed as follows:

$$F = W = \frac{\pi}{2}(1.19y)^2\cot^2\beta\left(1 - \frac{\tan\tau}{2\tan\beta}\right)\rho V^2 C_g \sin\tau + \frac{\rho g y^3}{3\sin\tau\tan\beta} \quad (22)$$

For cases in which the buoyant force is small as compared with the inertia force — that is, at high Froude numbers — the last term is neglected and C_g, which is in the first term, is equal to unity.

The vertical water reaction for the planing wedge with chines immersed is defined as follows:

$$F = W = \frac{\pi}{2}(1.19Z\cos\tau)^2\cot^2\beta\left[1 - \frac{Z\sin\tau\left(y - \frac{Z}{2}\right)}{y^2\tan\beta}\right]\rho V^2\sin\tau\, C_g$$

$$+ C_s\frac{\rho Z}{\tan\beta}V^2(y - Z\cos\tau)\sin\tau\cos\tau + \frac{\rho g Z}{\sin\tau\tan\beta}\left(y^2 - Zy + \frac{Z^2}{3}\right) \quad (23)$$

The correction factor C_g has not been defined mathematically but is presented in figure 8 in the form of empirical curves with a function of Froude number as a parameter. The dead-rise correction factor for the steady-flow force C_s is presented in table I.

CONCLUSIONS

An analysis has been made of planing data covering a wide range of dead-rise angles, trims, speeds, and beam loadings. The following conclusions are based on the results of the analysis:

1. The computation of the two-dimensional apparent additional mass at the step is based on the mass of water contained in a cylinder having a cross-sectional area of $1.42\frac{\pi}{2}\left(\frac{B}{2}\right)^2$ where B is the beam of the float.

2. Empirical gravity correction factors are applied at low Froude numbers to the inertia force which is fundamentally the product of the two-dimensional apparent additional mass at the step, the term $V^2 \sin \tau \cos^2 \tau$ (where V is horizontal velocity and τ is trim), and Pabst's correction factor for end losses.

3. The buoyant force is equal to the weight of the volume of water included between the immersed planing plate and the plane of level water where the pressure on the end area is neglected.

4. Bobyleff's correction factor is multiplied by the vertical component of the steady-flow forces which arise from the dynamic pressure of the stream impinging normal to the keel upon the area which is submerged behind the intersection of the chines with the level water surface.

5. Planing tests appear to be useful in aiding in the experimental verification of the theoretical nondimensional mass coefficients which are used in impact theory. Furthermore, these tests present a ready means of obtaining data which may be used in refining the coefficients so as to make them applicable over a wide range of float geometry and test conditions.

6. The planing coefficients and empirical gravity correction factors which are included in the resultant equations may be substituted directly in the general hydrodynamic-impact-load equations for angles of dead rise between 10° and 30° if the buoyant and steady-flow forces are used in the same form presented in the planing analysis and if the effect of gravity at different Froude numbers, indicated by the analysis of planing data, is assumed to be unaffected by the accelerations which occur in the impact case.

Langley Aeronautical Laboratory
National Advisory Committee for Aeronautics
Langley Field, Va., May 14, 1948

REFERENCES

1. Mayo, Wilbur L.: Analysis and Modification of Theory for Impact of Seaplanes on Water. NACA Rep. No. 810, 1945.

2. Milwitzky, Benjamin: A Generalized Theoretical and Experimental Investigation of the Motions and Hydrodynamic Loads Experienced by V-Bottom Seaplanes during Step-Landing Impacts. NACA TN No. 1516, 1948.

3. Lamb, Horace: Hydrodynamics. Sixth ed., Cambridge Univ. Press, 1932 pp. 104-105.

4. Shoemaker, James M.: Tank Tests of Flat and V-Bottom Planing Surface NACA TN No. 509, 1934.

5. Parkinson, John B.: A Complete Tank Test of a Model of a Flying-Boat Hull - N.A.C.A. Model No. 11-A. NACA TN No. 470, 1933.

6. King, Douglas A., and Hill, Mary B.: General Tank Tests of a $\frac{1}{10}$-Size Model of the Hull of the Boeing XPBB-1 Flying Boat - Langley Tank Model 175. NACA TN No. 1057, 1946.

7. Sottorf, W.: Experiments with Planing Surfaces. NACA TM No. 739, 1934.

TABLE I

BOBYLEFF'S DEAD-RISE CORRECTION FACTOR FOR STEADY-FLOW TERM

β (deg)	C_s (a)
10	0.844
15	.823
20	.800
$22\frac{1}{2}$	.790
24	.771
30	.750
40	.667

[a]These values are based on and interpolated from values obtained from reference 3, page 105.

TABLE II

GEOMETRIC PROPERTIES OF PLANING PLATES OR FLOATS

Reference	b (ft)	l_{max} (ft) (a)	β (deg)	Z (ft)
4	1.33	6.0	10	0.1180
			20	.2425
			30	.3850
5	1.417	2.0	$22\frac{1}{2}$	.292
7	.9843	All lengths usable	10	.087
			15	.132
			24	.219
			40	.4125
Recent tests in Langley tank no. 2	.835	3.33	20	.167

[a]Maximum length along the flat keel.

TABLE III

RECENT DATA OBTAINED IN TESTS IN LANGLEY TANK NO. 2

WITH A V-SHAPED PLANING PLATE

[$\beta = 20^\circ$; $\tau = 6^\circ$]

W (lb)	V (fps)	y (ft)
5	10	0.137
	20	.066
	30	.045
	40	.038
	50	.033
10	10	.213
	20	.092
	30	.065
	40	.052
20	10	.307
	20	.133
	30	.088
	40	.068
	50	.058
40	20	.253
	30	.130
	40	.093
	50	.080
50	20	.323
	30	.158
	40	.108
	50	.087

NACA

TABLE IV

DRAFT MEASUREMENTS OBTAINED FROM REFERENCE 7

β (deg)	τ (deg)	l (ft) (a)	y (ft)
10	4	3.42	0.239
	6	1.83	.190
	8	1.09	.152
15	4	3.70	.259
	6	2.12	.222
	8	1.28	.178
24	4	4.38	.307
	6	2.60	.271
	8	1.75	.244
40	4	6.1	.428
	6	4.3	.450
	8	3.1	.430

[a]Obtained from figures 20 to 23, reference 7.

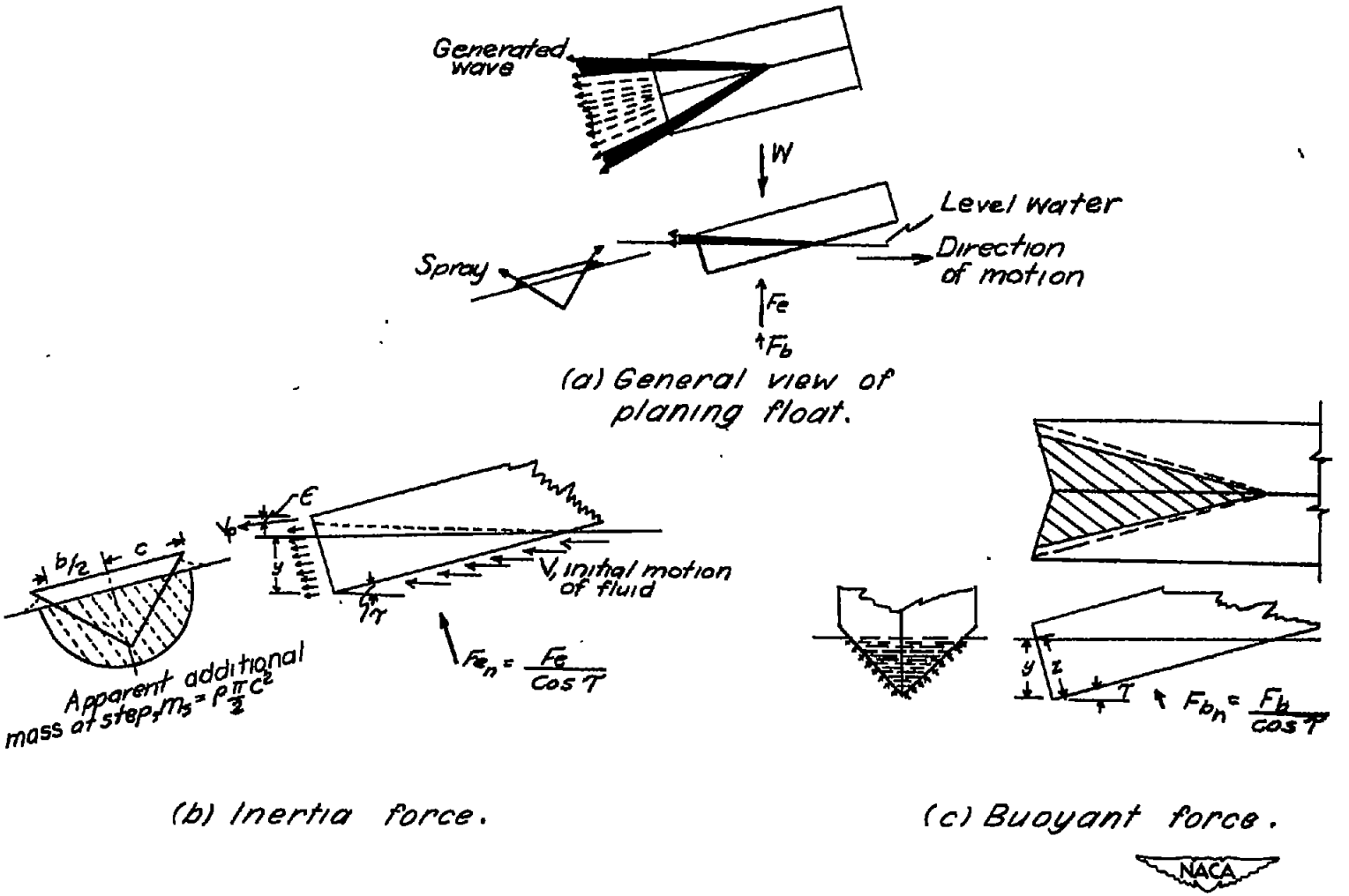

Figure 1.— Planing float with chines above level water.

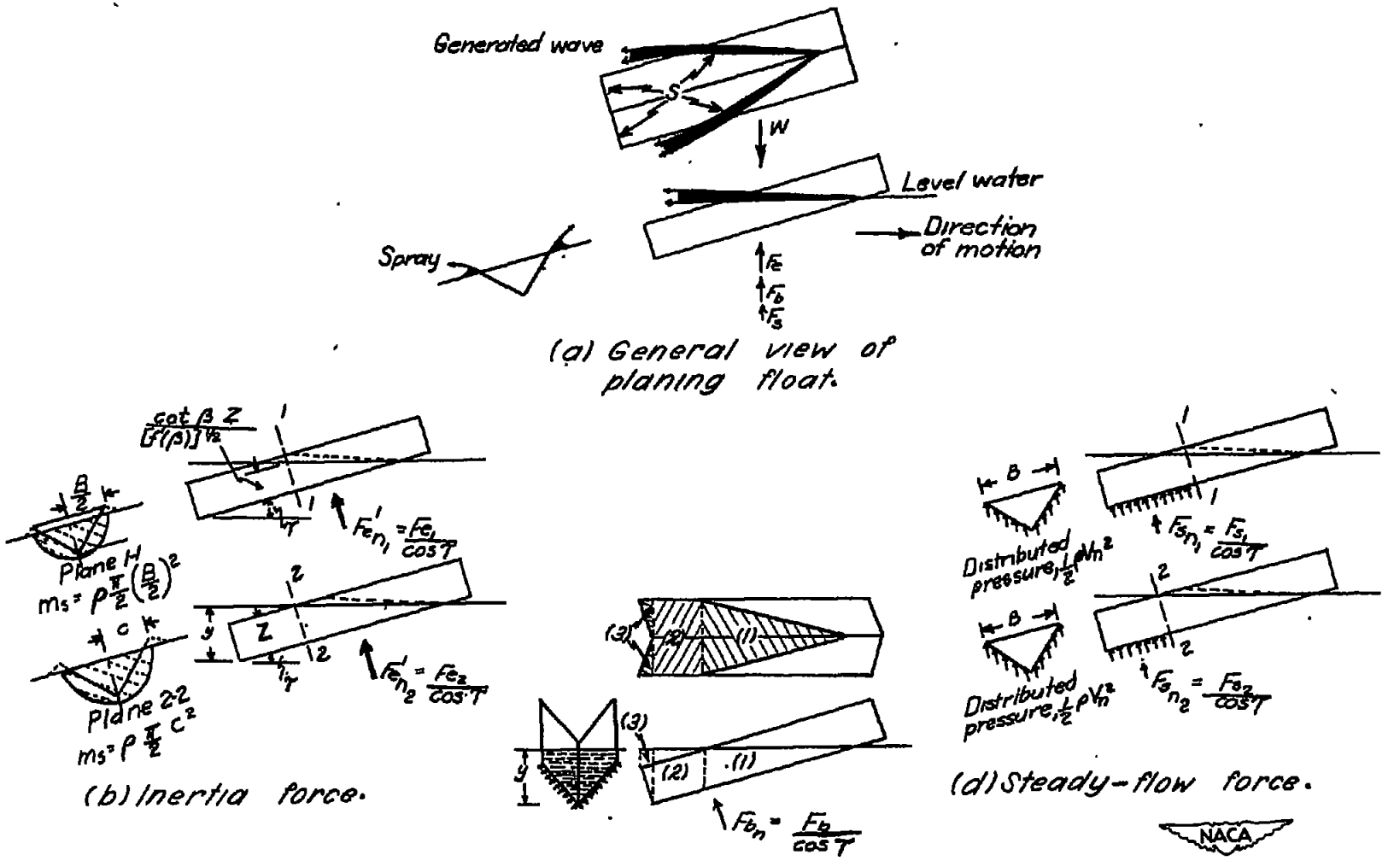

Figure 2.—Planing float with chines immersed.

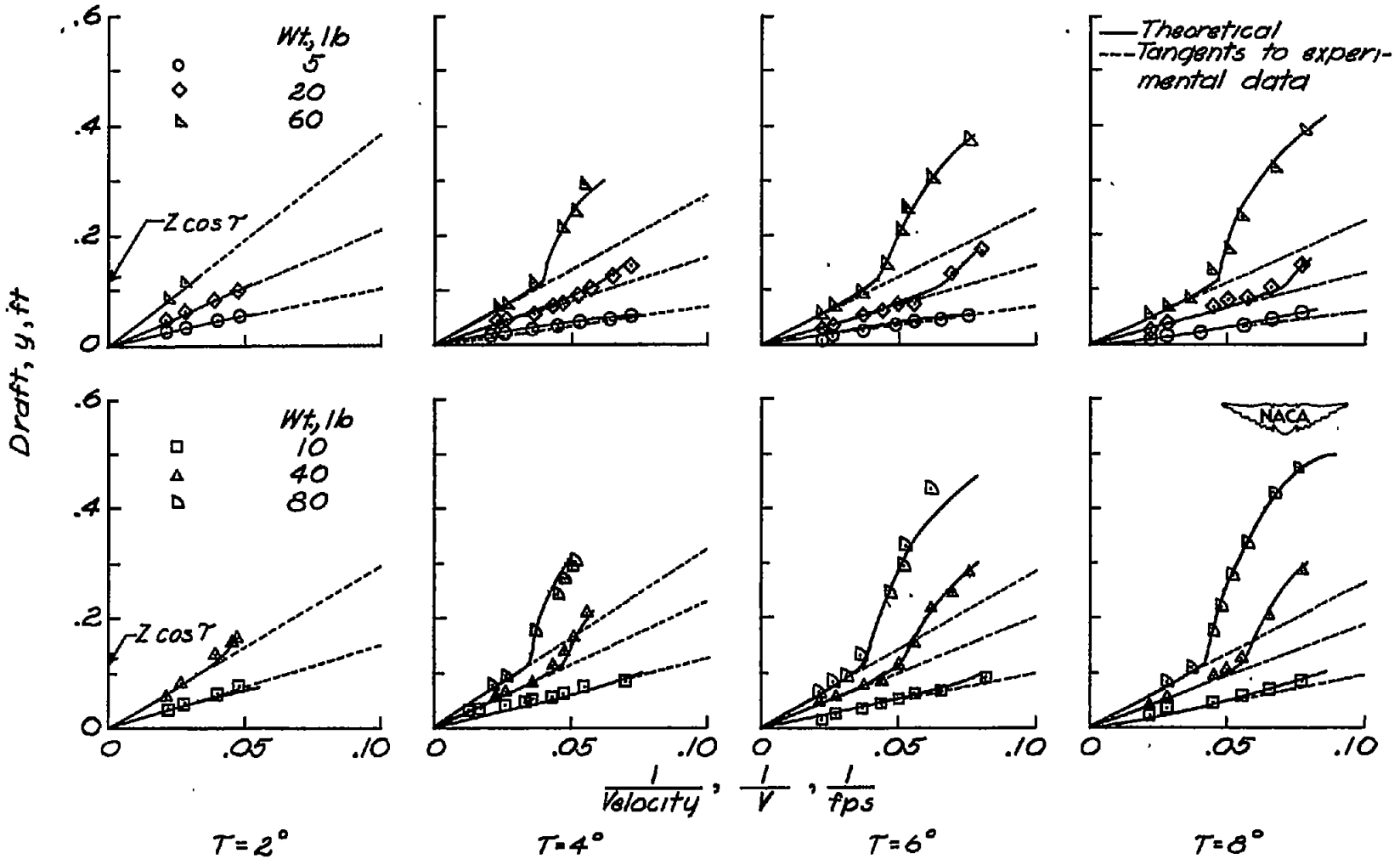

(a) Planing plate with 10° dead-rise angle.

Figure 3. — Variation of draft with velocity for a planing wedge having triangular cross section.

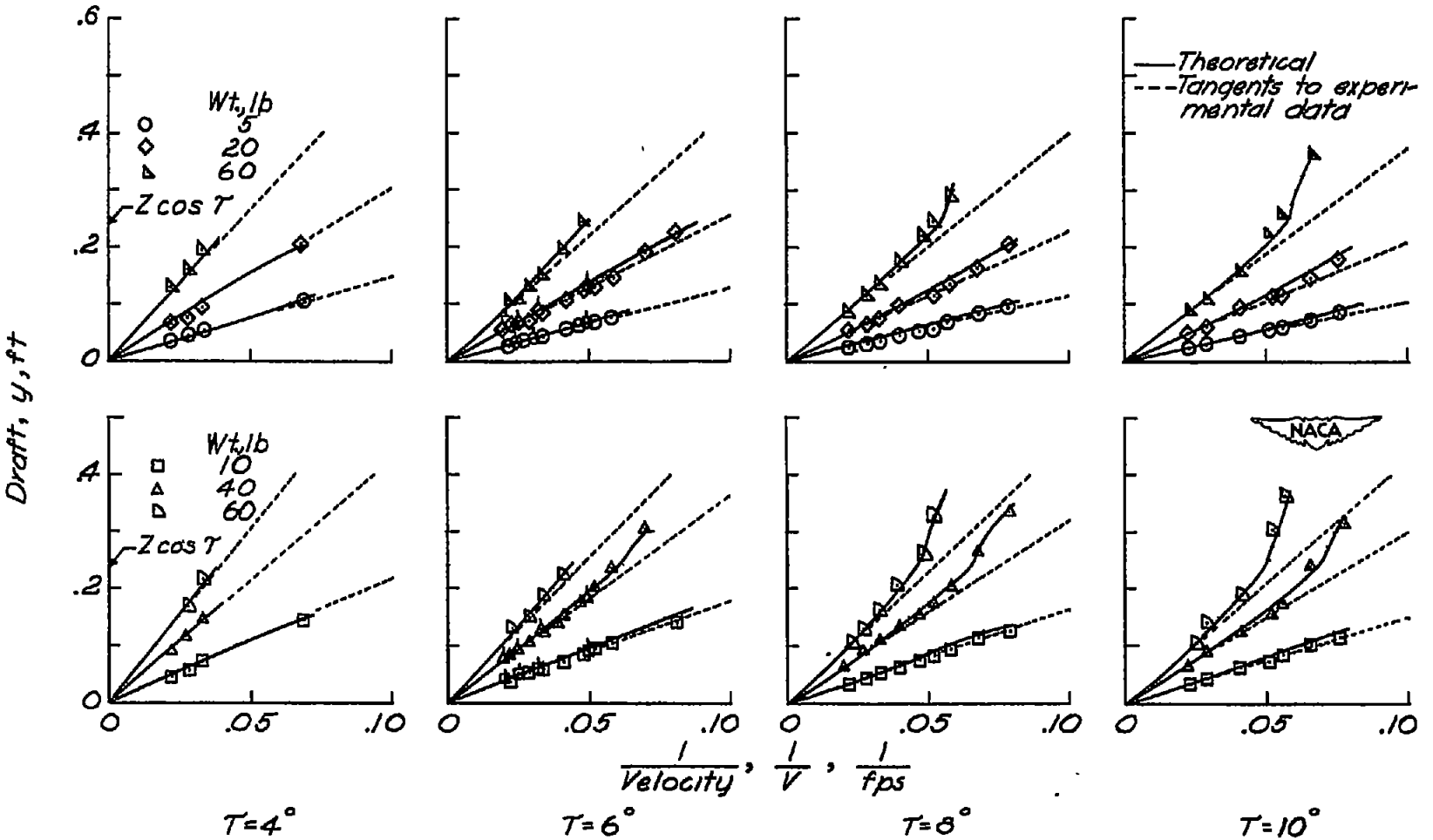

(b) Planing plate with 20° dead-rise angle.

Figure 3. — Continued.

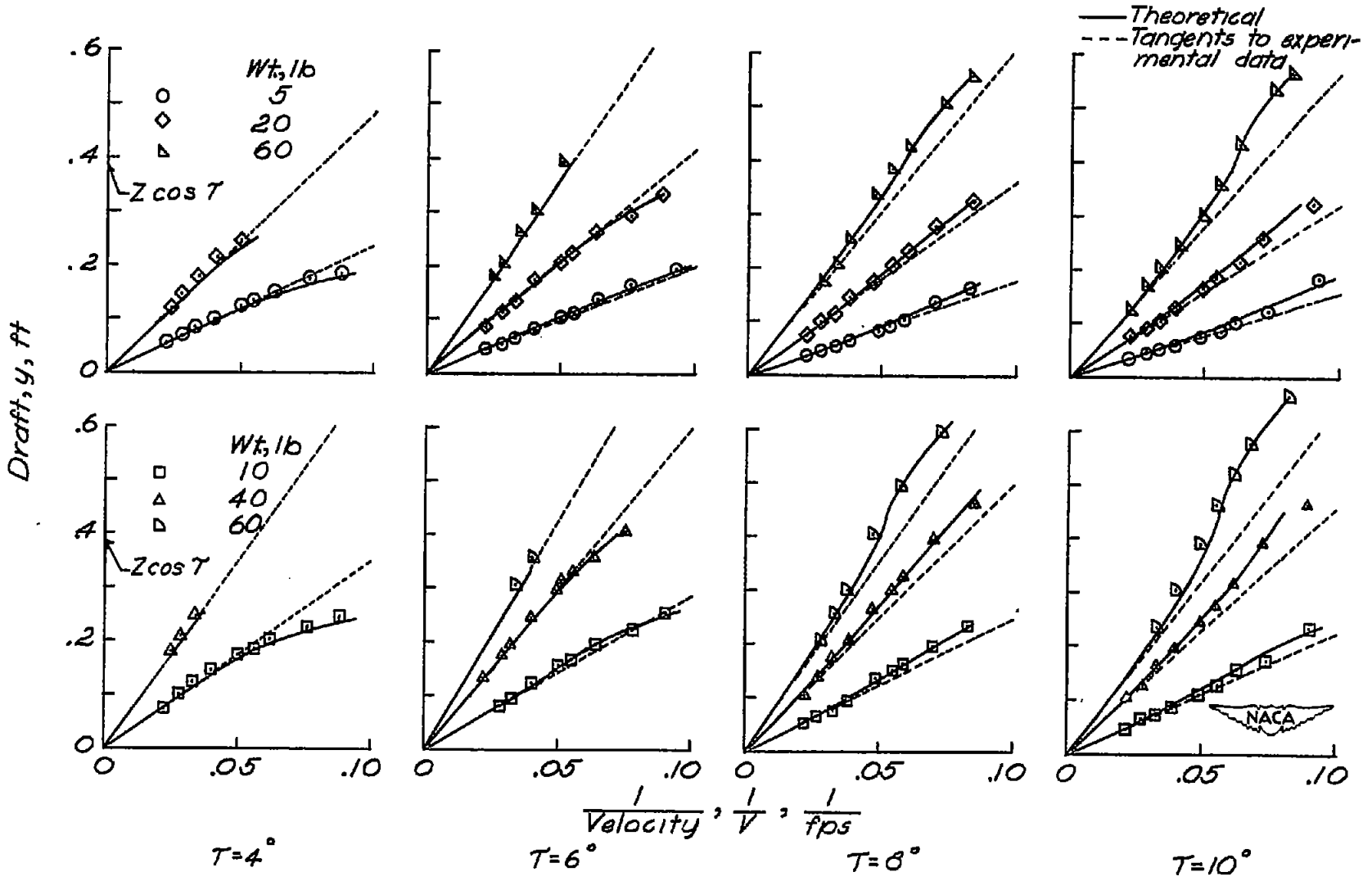

(c) Planing plate with 30° dead-rise angle.

Figure 3.—— Continued.

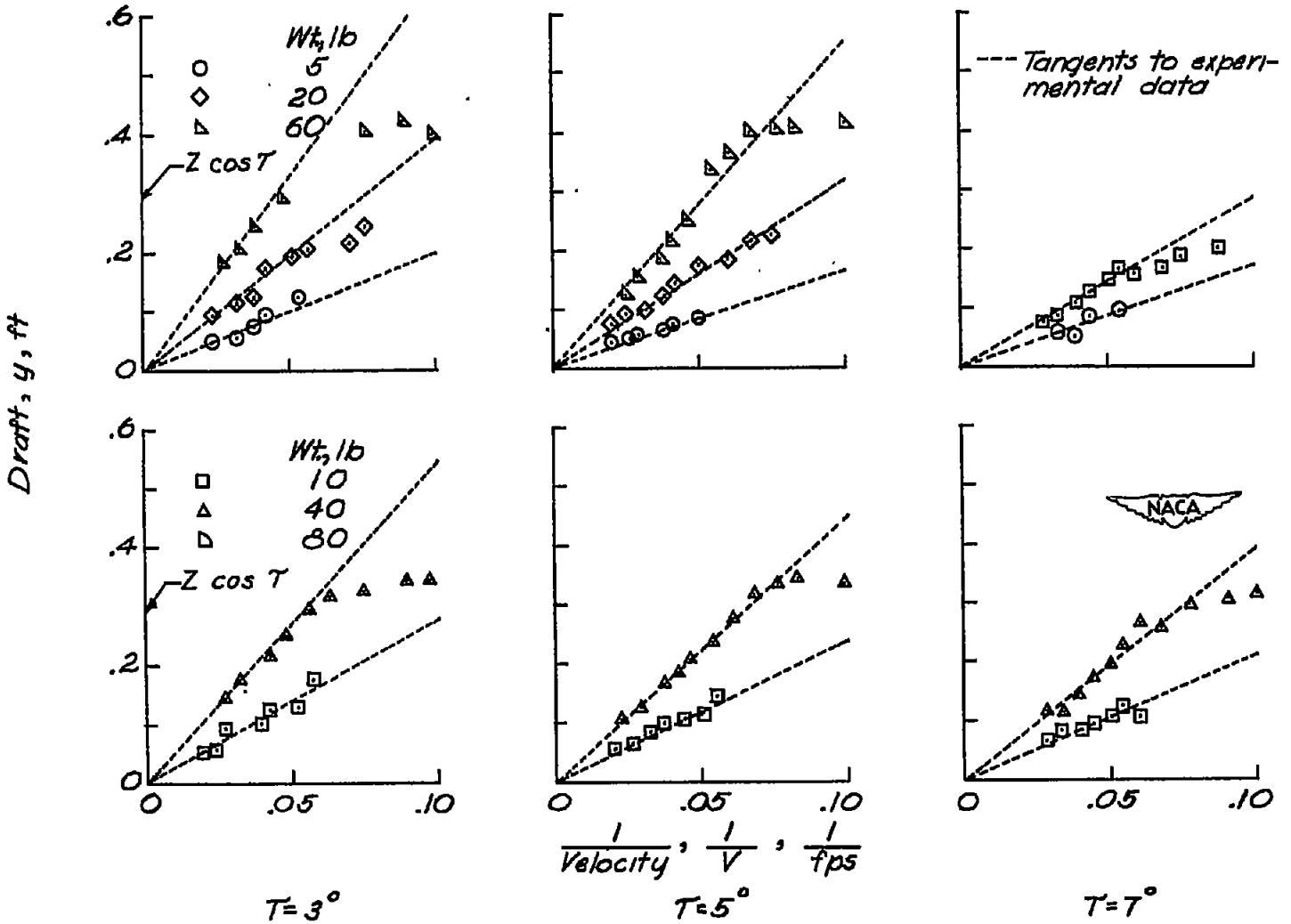

(d) Planing plate with $22\frac{1}{2}^{\circ}$ dead-rise angle.

Figure 3. — Concluded.

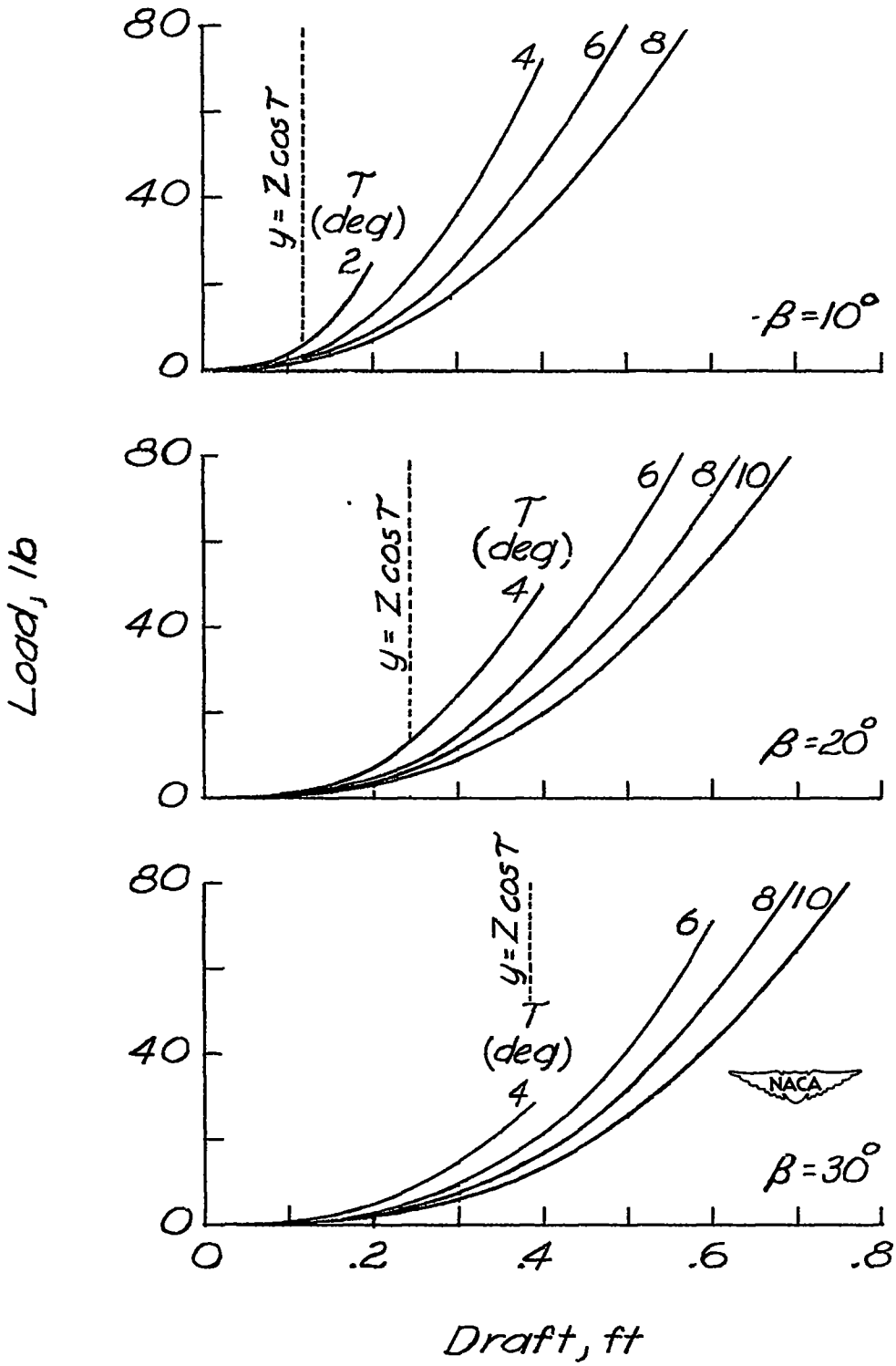

Figure 4.— Buoyant forces on planing plates. Beam = 1.33 feet.

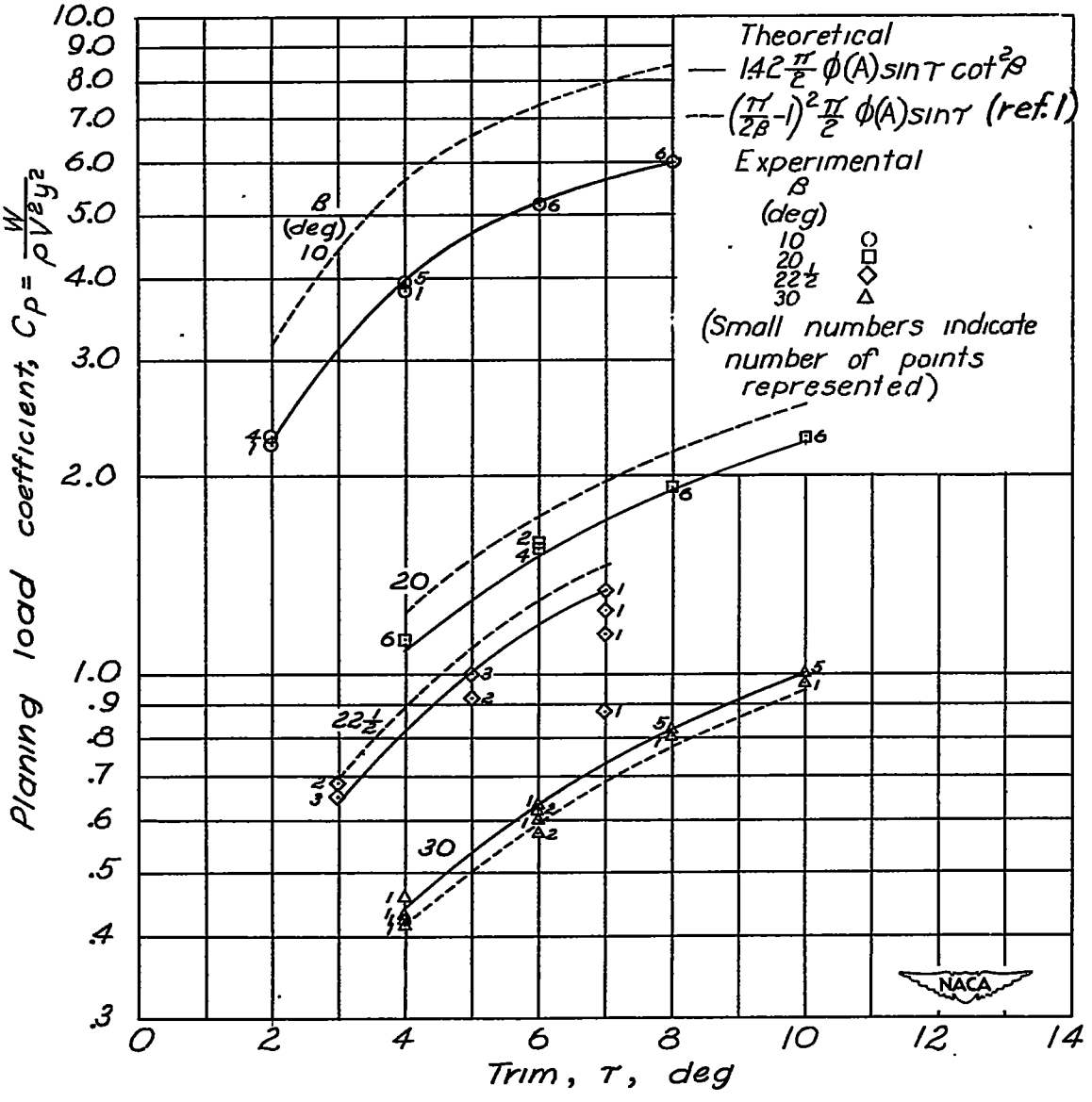

Figure 5. —— Comparison of theoretical and experimental planing coefficients. Buoyant forces omitted.

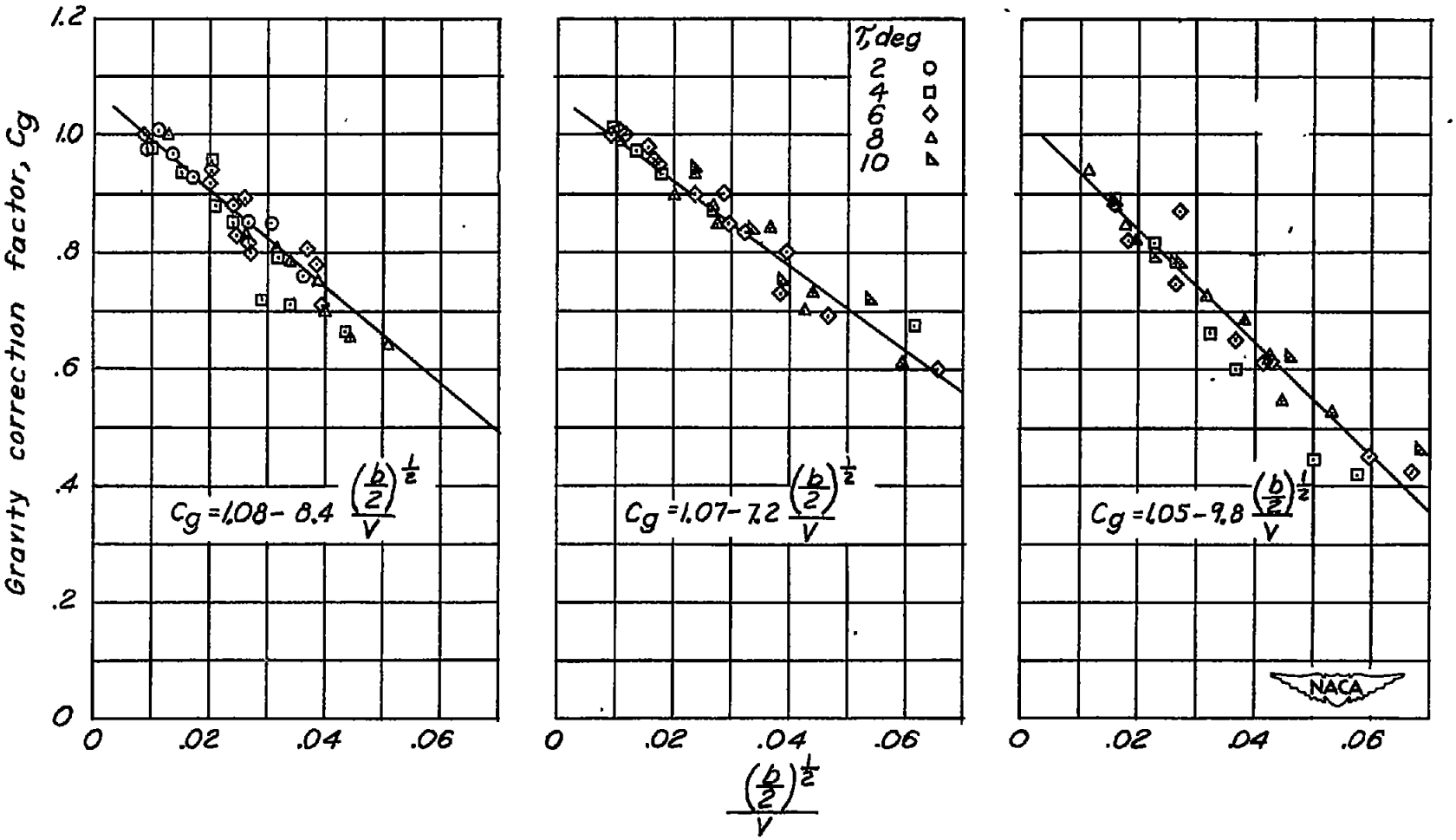

(a) $\beta = 10°$. (b) $\beta = 20°$. (c) $\beta = 30°$.

Figure 6.- Empirical gravity correction curves, chines above level water.

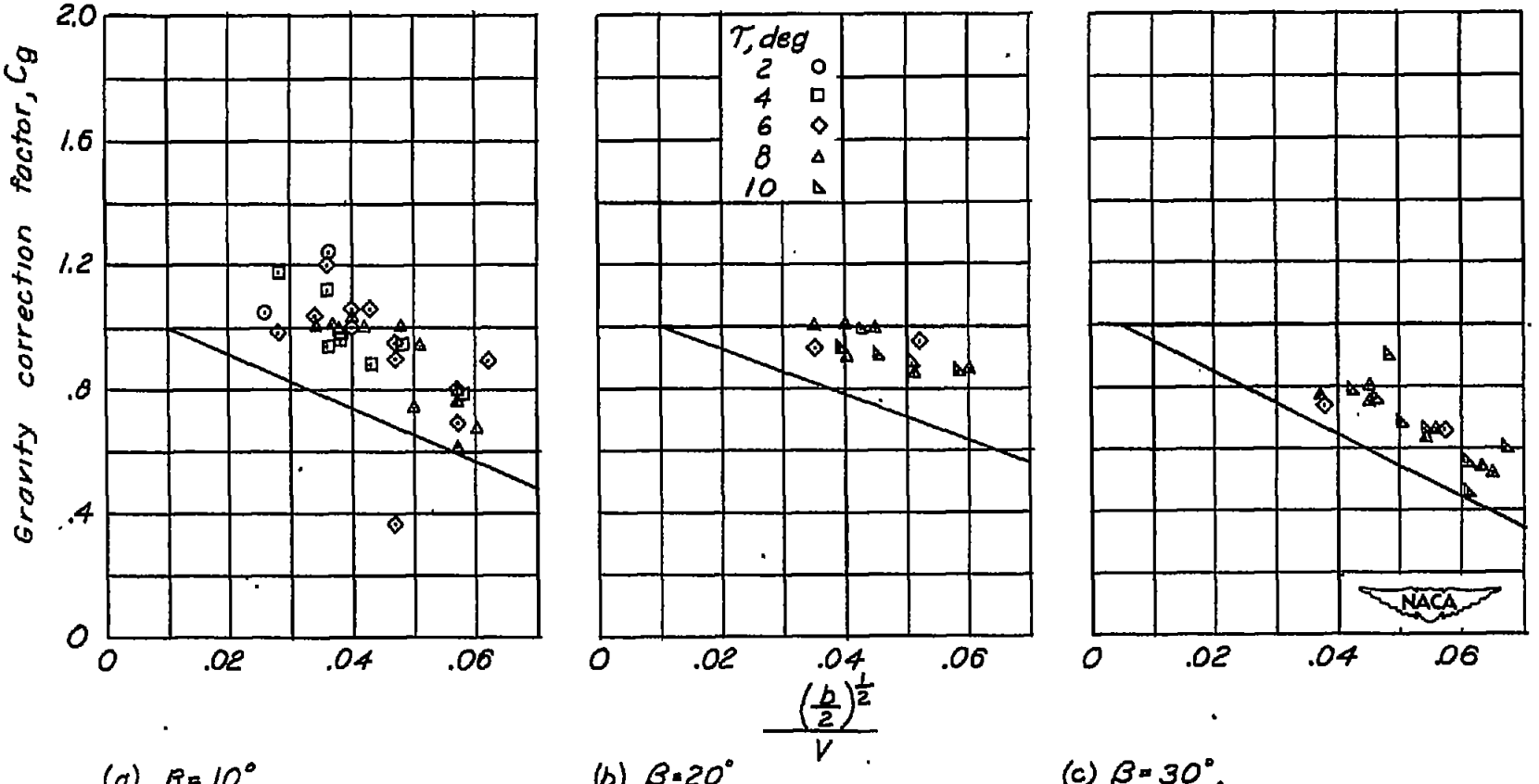

(a) $\beta = 10°$. (b) $\beta = 20°$. (c) $\beta = 30°$.

Figure 7. – Comparison of empirical correction factors for chine immersion with correction curves for chines above level water.

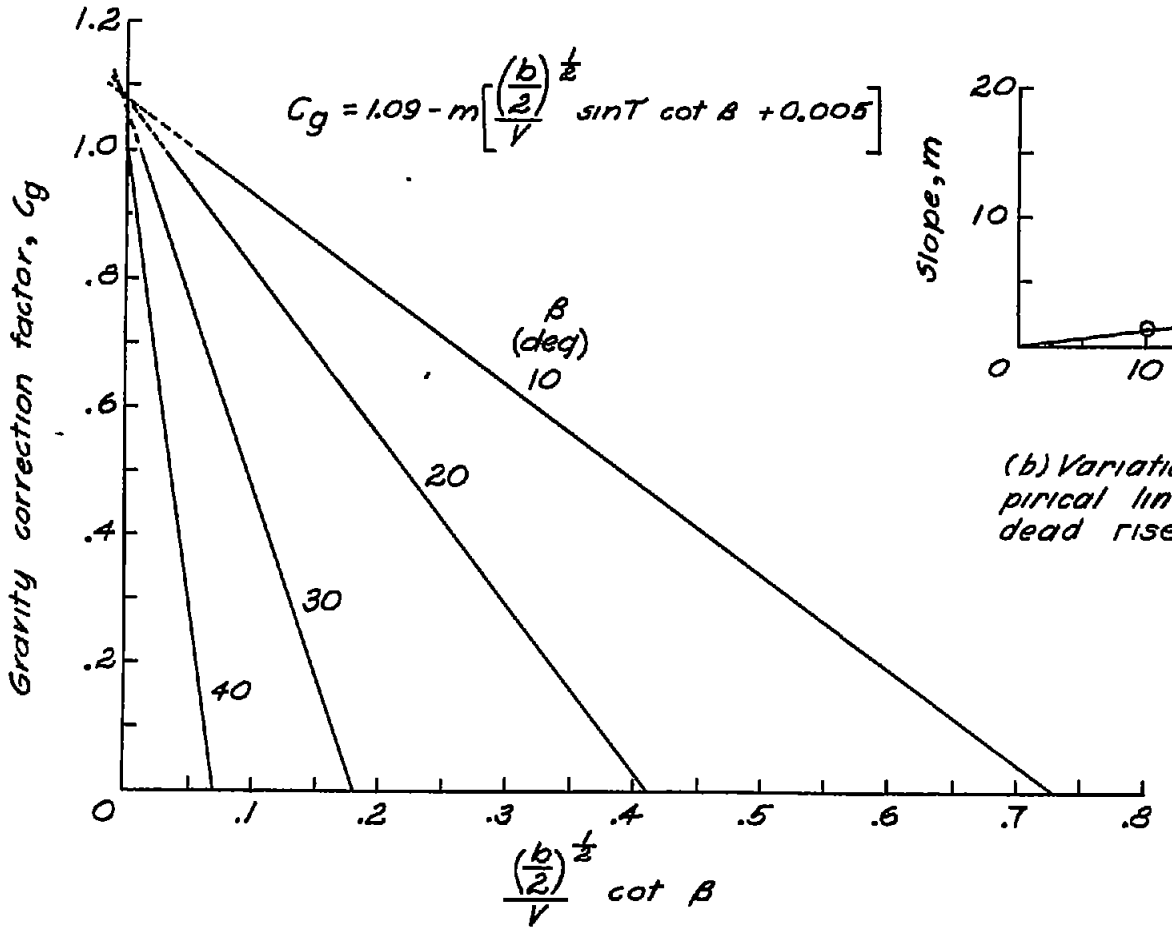

(a) Converted empirical correction lines.

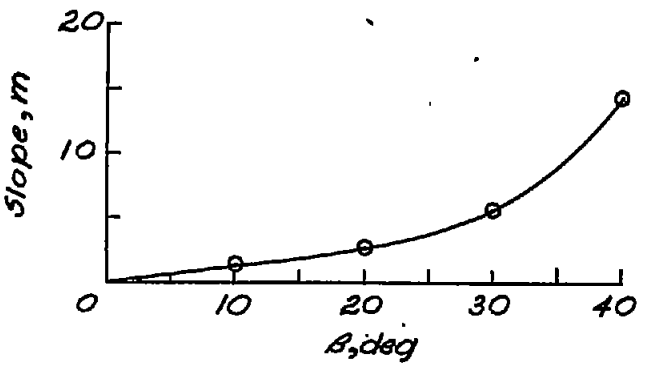

(b) Variation of slope of empirical lines with angle of dead rise.

Figure 8. — Empirical gravity correction curves indicated by the analysis of planing data.

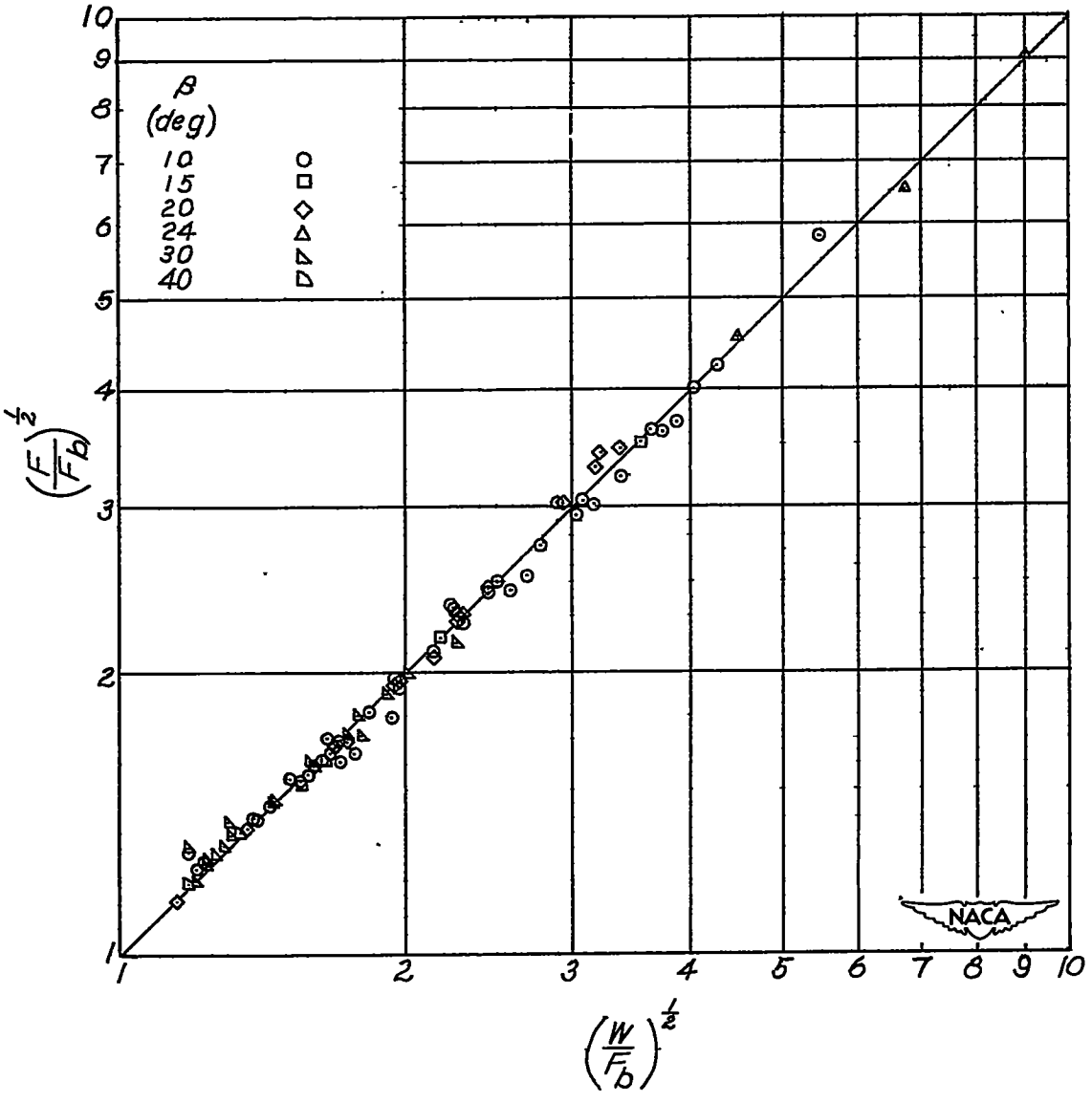

Figure 9.—— Comparison between experimental and computed vertical planing load on a wedge with chines immersed.